

THE TOPOLOGICAL-SHAPE SENSITIVITY ANALYSIS AND ITS APPLICATIONS IN OPTIMAL DESIGN

Raúl A. Feijóo*, Antonio A. Novotny*, Claudio Padra†
and
Edgardo O. Taroco*

*Laboratório Nacional de Computação Científica, LNCC
Ministério de Ciência e Tecnologia, MCT
Av. Getúlio Vargas 333, Quitandinhas, 25651-070 Petrópolis, Rio de Janeiro, Brasil
e-mail: feij@lncc.br, novotny@lncc.br, etam@lncc.br

†Centro Atómico Bariloche, Grupo de Mecánica Computacional
8400 Bariloche, Argentina
e-mail: padra@cab.cnea.gov.ar

Key Words: Topological Optimization, Shape Sensitivity Analysis, Elasticity, Heat Conduction.

Abstract. *The Topological Derivative concept has been seen as a powerful framework to obtain the optimal domain topology for several engineering problems. This derivative is a function defined in a domain, which characterizes the sensitivity of the problem when a small hole is created at each point of it. However, the greatest limitation of this methodology is that when a hole is created it is impossible to build a homeomorphic map between the domains in study (because they have not the same topology). Therefore, some specific mathematical framework should be developed in order to obtain the derivatives. This work proposes an alternative way to compute the Topological Derivative based on the Shape Sensitivity Analysis concepts, which has been denoted as the **Topological-Shape Sensitivity Analysis**. The main feature of this methodology is that all the mathematical procedure already developed in the context of Shape Sensitivity Analysis may be used in the calculus of the Topological Derivative. This idea leads to a more simple and constructive formulation than the ones found in the literature. Further, to point out the straightforward use of the proposed methodology, it is applied for solving some Topological Optimization problems for several problems in steady-state heat conduction and 2D elasticity.*

1 INTRODUCTION

Many physics phenomena can be modeled by a set of partial differential equations with proper boundary conditions (boundary-value problem) or by its equivalent weak form defined over a certain domain. A question of great importance, that has awoken a lot of interest in recent years, is the ability to obtain automatically, in agreement with some measure of performance (cost function), the optimal geometry of the domain of definition of the problem under analysis. Conceptually, the problem is to find the domain, *i.e.* its shape and/or topology such that the cost functional is minimized with the constraints imposed by the boundary-value problem. An already established method in the literature that addresses this kind of problems is to parameterize the domain of interest followed by an optimization with respect to these parameters. This leads to the well-known shape optimization technique. The inconvenience of this approach is that the topology is fixed throughout the optimization process. In order to overcome this limitation, topological optimization techniques were developed where very little is assumed about the initial morphology of the domain. The main advantage of this methodology is that the optimal topology can be obtained even from an initial configuration that is far away from the optimal one.

Important contributions in the field of topology optimization have been obtained by characterizing the topology as a material density to be determined. In these methodologies the cavities correspond to a region of zero density while the domain is identified by the region where the density is non-zero. This approach is based in the concepts of relaxed formulations and homogenization techniques (see, for instance, Bendsoe & Kikuchi¹), where, in order to obtain different densities throughout the domain, a class of micro cells of laminated material is introduced and an homogenization method is used to compute the physical properties of these microstructures. Therefore, the optimal solution may be seen as a distribution of fictitious materials that compose the domain. Finally, penalization methods and filtering techniques are needed to retrieve the feasible design. This overall approach leads to results that may be far away from the optimal one.

The work of Souza de Cursi² presents a topological optimization method for structural components in the elastic linear regime. In this work, structures with minimum mass and stresses below the von Mises plastic failure threshold are searched. The basic idea of this formulation consists in the characterization of the morphology of the structure using a geometric parameter ρ such that, for $\rho > 0$, one achieves saturation of the von Mises yield criteria (*fully stressed design condition*). On the other hand, for $\rho = 0$ one obtains a cavity in the domain. A limitation of this methodology is that it is necessary to establish a mathematical formulation where the thickness map ρ appears explicitly as a multiplying parameter in the state equations.

Finally, in these works (and references there in) only homogeneous natural boundary conditions on the contour of the cavities were considered. Other boundary conditions, such as non-homogeneous Neumann boundary conditions, Dirichlet (either homogeneous

or not) and Robin, are not trivial to be treated using these approaches, which is reflected by the absence of publications in this direction.

More recently, Schumacher³ and Garreau et al.^{4,5} presented a method to obtain the optimal topology by calculating the so-called Topological Derivative. The Topological Derivative is a function defined in the domain of interest where, at each point, it gives the sensitivity of the cost function when a small hole is created at that point. More specifically, the idea is to make a perturbation on the domain Ω by subtracting a ball of radius ϵ , denoted by B_ϵ , centered in a point $\mathbf{x} \in \Omega$. This originates a new domain $\Omega_\epsilon = \Omega - \overline{B}_\epsilon$. Therefore, if a cost function $\psi(\cdot)$ defined in Ω is considered, the Topological Derivative, here denoted by D_T^* , can be defined as

$$\psi(\Omega_\epsilon) = \psi(\Omega) + f(\epsilon)D_T^* + \mathcal{R}(f(\epsilon)). \tag{1}$$

In the expression above $f(\epsilon)$ is a negative function that depends on the problem under analysis and that monotonically decreases so that $f(\epsilon) \rightarrow 0$ when $\epsilon \rightarrow 0$. $\mathcal{R}(f(\epsilon))$ contains all higher order terms than $f(\epsilon)$, that is, it satisfies

$$\lim_{\epsilon \rightarrow 0} \frac{\mathcal{R}(f(\epsilon))}{f(\epsilon)} = 0.$$

In general, ψ depends explicitly and implicitly on ϵ . The implicit dependence arises from the solution of a partial differential equation defined in Ω_ϵ . If this equation is elliptic, conditions in the whole boundary of Ω_ϵ must be imposed. Therefore, when \overline{B}_ϵ is introduced, boundary conditions must also be defined on ∂B_ϵ .

Using the Dirichlet-to-Neumann map, an asymptotic analysis of the above problem was carried out by Garreau et al.^{4,5}. This methodology, called the Domain Truncation Method, has shown that the term that dominates the development of (1) is given by D_T^* . Furthermore, it can be used for singular problems such as those with Dirichlet boundary conditions imposed on ∂B_ϵ .

The Topological Derivative concept has been regarded as a powerful tool to solve topological optimization problems where no restrictions concerning the nature of the phenomena as well as the boundary conditions imposed on the holes are made. However, according to the approach adopted in the referenced works, this quite general concept can become restrictive, due to mathematical difficulties involved in the calculation of the Topological Derivative. In fact, the work of Garreau et al.⁴ introduced several simplification hypothesis. For example, the cost function was assumed to be independent of the domain, only homogeneous Dirichlet and Neumann boundary conditions on the holes were considered, the source terms of the boundary value problem were assumed to be constant.

On the other hand, Shape Sensitivity Analysis, which has been shown to be a powerful tool to only solve shape optimization problems, was proposed by Sokolowski and Zochowski⁶ and C ea et al.⁷ as an alternative way to evaluate the Topological Derivative.

Nevertheless, their theory yields correct results only for some particular cases (for example, homogeneous Neumann boundary conditions on the hole). Moreover, in these works, the relation between both concepts was stated heuristically, remaining an open question.

More recently, in Novotny et al.^{8–10} and Feijóo et al.¹¹, was formally established the relation between the Topological Derivative and the Shape Sensitivity Analysis concepts. This novel methodology, called by the authors **Topological-Shape Sensitivity Analysis** (TSSA) leads to a simple and constructive procedure to calculate the Topological Derivative, that can be applied for a large class of linear and non-linear Engineering problems. Both homogeneous and non-homogeneous versions of Dirichlet, Neumann and Robin boundary conditions were considered on ∂B_ϵ .

With these ideas in mind, the Topological-Shape Sensitivity Analysis (TSSA) is reviewed and applied in several topological optimization design problems. The Section 2 briefly recalls the Topological-Shape Sensitivity Analysis theory, whose fundamental result is given in the TSSA Theorem (Eq. 7). Next, in Sections 3 and 4, this result is applied to 2D heat conduction and elasticity problem respectively, considering different boundary conditions on the hole. Finally, to point out the potentiality of the proposed methodology, in Section 5 some numerical results in the topological optimization context are presented.

2 THE TOPOLOGICAL-SHAPE SENSITIVITY ANALYSIS

Let $\Omega \subset \mathbb{R}^2$ be an open bounded domain, whose boundary Γ is smooth enough, *i.e.* a unit normal vector \mathbf{n} exist almost everywhere. Let still $\Omega_\epsilon \subset \mathbb{R}^2$ be a new domain, such that $\Omega_\epsilon = \Omega - \overline{B}_\epsilon$, whose boundary is denoted by $\Gamma_\epsilon = \Gamma \cup \partial B_\epsilon$, where $\overline{B}_\epsilon = B_\epsilon \cup \partial B_\epsilon$ is a ball of radius ϵ centered on the point $\hat{\mathbf{x}} \in \Omega$. Considering a cost function $\psi(\cdot)$ defined in a certain domain, then the Topological Derivative is defined as⁴

$$D_T^*(\hat{\mathbf{x}}) := \lim_{\epsilon \rightarrow 0} \frac{\psi(\Omega_\epsilon) - \psi(\Omega)}{f(\epsilon)}, \quad (2)$$

where $f(\epsilon)$ is a negative function that decreases monotonically so that $f(\epsilon) \rightarrow 0$ with $\epsilon \rightarrow 0$ ($0 \leq \epsilon < 1$). It is important to mention that the derivative given by Eq. (2) cannot be obtained in a conventional way because Ω_ϵ and Ω have not the same topology, *i.e.* it is impossible to build an homeomorphism between these domains.

Therefore, the idea behind the Topological-Shape Sensitivity Analysis is to start from a problem in that the hole \overline{B}_ϵ already exists, *i.e.* from Ω_ϵ , causing a small perturbation $\delta\epsilon$ in the \overline{B}_ϵ , in order to originate a new domain $\Omega_{\epsilon+\delta\epsilon} = \Omega - \overline{B}_{\epsilon+\delta\epsilon}$, whose boundary is written as $\Gamma_{\epsilon+\delta\epsilon} = \Gamma \cup \partial B_{\epsilon+\delta\epsilon}$. Thus, the Topological Derivative can be redefined as

$$D_T(\hat{\mathbf{x}}) := \lim_{\epsilon \rightarrow 0} \left\{ \lim_{\delta\epsilon \rightarrow 0} \frac{\psi(\Omega_{\epsilon+\delta\epsilon}) - \psi(\Omega_\epsilon)}{f(\epsilon + \delta\epsilon) - f(\epsilon)} \right\}. \quad (3)$$

The advantage of this last definition (Eq. 3) is that the whole mathematical framework developed for the Shape Sensitivity Analysis can be used to compute the Topological

Derivative. Indeed, considering that the domain Ω_ϵ suffers a perturbation, which can be represented by a smooth and invertible mapping dependent on the parameter τ , in the following manner

$$\chi(\mathbf{x}, \tau) : \mathbf{x} \mapsto \mathbf{x}_\tau \quad \forall \mathbf{x} \in \Omega_\epsilon \subset \mathbb{R}^2, \tag{4}$$

then, the perturbed domain Ω_τ as well as its boundary Γ_τ , can be described, respectively, as

$$\begin{aligned} \Omega_\tau &:= \{ \mathbf{x}_\tau \in \mathbb{R}^2 \mid \exists \mathbf{x} \in \Omega_\epsilon, \mathbf{x}_\tau = \chi(\mathbf{x}, \tau), \mathbf{x}_\tau|_{\tau=0} = \mathbf{x}, \Omega_\tau|_{\tau=0} = \Omega_\epsilon \}, \\ \Gamma_\tau &:= \{ \mathbf{x}_\tau \in \mathbb{R}^2 \mid \exists \mathbf{x} \in \Gamma_\epsilon, \mathbf{x}_\tau = \chi(\mathbf{x}, \tau), \mathbf{x}_\tau|_{\tau=0} = \mathbf{x}, \Gamma_\tau|_{\tau=0} = \Gamma_\epsilon \}. \end{aligned}$$

where, for τ small enough, every point \mathbf{x}_τ may be written as $\mathbf{x}_\tau = \mathbf{x} + \tau \mathbf{V}$, being \mathbf{V} the *velocity of change of form*^{12,13}.

Thus, the (shape) sensitivity of the cost function $\psi(\Omega_\tau)$ in relation to the domain perturbation, characterized by τ , is given by the following derivative

$$\left. \frac{d}{d\tau} \psi(\Omega_\tau) \right|_{\tau=0} = \lim_{\tau \rightarrow 0} \frac{\psi(\Omega_\tau) - \psi(\Omega_0)}{\tau}. \tag{5}$$

Remembering that only the ball \overline{B}_ϵ suffers a perturbation $\delta\epsilon$, so $\Omega_{\epsilon+\delta\epsilon} = \Omega_\tau$ and $\Gamma_{\epsilon+\delta\epsilon} = \Gamma_\tau$ and considering a suitable velocity field along the boundary $\Gamma_\epsilon = \Gamma \cup \partial B_\epsilon$, such that

$$\begin{cases} \mathbf{V} = V_n \mathbf{n} & \text{with } V_n < 0 \text{ constant on } \partial B_\epsilon \\ \mathbf{V} = 0 & \text{on } \Gamma \end{cases}, \tag{6}$$

then, it is possible to establish the relation between the Topological Derivative and the Shape Sensitivity Analysis concepts, through the following theorem

Topological-Shape Sensitivity Analysis Theorem (TSSA Theorem)^{9,11}: Let $f(\epsilon)$ be a function chosen in order to $0 < |D_T^*(\hat{\mathbf{x}})| < \infty$, then the limit with $\epsilon \rightarrow 0$ that appears in the definition of the Topological Derivative given by Eq. (2) can be written as

$$D_T^*(\hat{\mathbf{x}}) = D_T(\hat{\mathbf{x}}) = \lim_{\epsilon \rightarrow 0} \frac{1}{f'(\epsilon) |V_n|} \left. \frac{d}{d\tau} \psi(\Omega_\tau) \right|_{\tau=0}. \tag{7}$$

This theorem points out that the Topological Derivative may be obtained through the Shape Sensitivity Analysis of the cost function. Therefore, results obtained in Shape Sensitivity Analysis, whose mathematical foundation is already well developed¹⁴, can be used to calculate the Topological Derivative in a simple and constructive way given by the expression (7).

3 TOPOLOGICAL DERIVATIVE IN THE POISSON'S PROBLEM

To illustrate the potentialities of the result of the TSSA Theorem, the Topological Derivative will be calculated, utilizing the Eq. (7), in the problem of steady-state energy transfer in two-dimensional rigid bodies. It is important to mention that the extension to three-dimensional domains is straightforward to consider. From the equations of the first law of

thermodynamics (energy balance) in permanent regime and considering the constitutive equation given by the Fourier's law for isotropic materials, one has a problem that may be modeled by a second order elliptic boundary value problem, classically known as the Poisson's equation (see, for instance, Carlson¹⁵ or Slattery¹⁶). On the holes, boundary conditions will be imposed either in the temperature (Dirichlet), in the heat flux (Neumann) or even in both variables (Robin). Physically, the holes can be interpreted as cooling channels, where the convection is totally predominant (prescribed temperature) or where there is a prescribed heat flux (thermal isolation, for example). A more realistic situation can be considered admitting a finite and non-null convection in the holes. Such a phenomenon can be modeled through the well-known Newton's law of cooling, leading to the mixed boundary conditions (Robin) on the holes.

3.1 Formulation of the problem

Let a rigid body be represented by $\Omega_\epsilon \subset \mathbb{R}^2$ with a small hole \overline{B}_ϵ centered in $\hat{x} \in \Omega$, whose boundary $\Gamma_\epsilon = \Gamma \cup \partial B_\epsilon$ is such that $\Gamma = \Gamma_N \cup \Gamma_D \cup \Gamma_R$, with $\Gamma_N, \Gamma_D, \Gamma_R, \partial B_\epsilon$ mutually disjoint. Considering that the body is submitted to a constant excitation b in the domain Ω_ϵ and Dirichlet (or essential), Neumann (or natural) and/or Robin (or mixed) boundary conditions on Γ_D, Γ_N and Γ_R , respectively, and that on the contour of the holes (on ∂B_ϵ), will also be imposed either Dirichlet, Neumann or Robin boundary conditions. Thus, the solution u_ϵ must satisfy the Poisson's equation, that is:

$$\left\{ \begin{array}{ll} \text{Find } u_\epsilon, \text{ such that} & \\ -k \Delta u_\epsilon = b & \text{in } \Omega_\epsilon \\ u_\epsilon = \bar{u} & \text{on } \Gamma_D \\ -k \frac{\partial u_\epsilon}{\partial n} = \bar{q} & \text{on } \Gamma_N \\ -k \frac{\partial u_\epsilon}{\partial n} = h_c (u_\epsilon - u_\infty) & \text{on } \Gamma_R \\ h(\alpha, \beta, \gamma) = 0 & \text{on } \partial B_\epsilon \end{array} \right. , \tag{8}$$

where the function $h(\alpha, \beta, \gamma)$ is such that:

$$h(\alpha, \beta, \gamma) = \alpha (u_\epsilon - \bar{u}^\epsilon) + \beta \left(k \frac{\partial u_\epsilon}{\partial n} + \bar{q}^\epsilon \right) + \gamma \left(k \frac{\partial u_\epsilon}{\partial n} + h_c^\epsilon (u_\epsilon - u_\infty^\epsilon) \right) = 0, \tag{9}$$

and $\alpha, \beta, \gamma \in \{0, 1\}$ with $\alpha + \beta + \gamma = 1$. Therefore, the three kind of boundary conditions on ∂B_ϵ considered in this work are obtained combining the parameters α, β and γ adequately, that is:

$$h(\alpha, \beta, \gamma) = \left\{ \begin{array}{ll} u_\epsilon - \bar{u}^\epsilon, & \text{if } \alpha = 1, \beta = \gamma = 0, \text{ Dirichlet} \\ k \frac{\partial u_\epsilon}{\partial n} + \bar{q}^\epsilon, & \text{if } \beta = 1, \alpha = \gamma = 0, \text{ Neumann} \\ k \frac{\partial u_\epsilon}{\partial n} + h_c^\epsilon (u_\epsilon - u_\infty^\epsilon), & \text{if } \gamma = 1, \alpha = \beta = 0, \text{ Robin} \end{array} \right. . \tag{10}$$

The parameters $k, \bar{u}, \bar{q}, u_\infty, h_c, \bar{u}^\epsilon, \bar{q}^\epsilon, u_\infty^\epsilon$ and h_c^ϵ are considered, for simplicity, constants in this work, where k is the thermal conductivity; \bar{u} is the prescribed temperature on Γ_D ; \bar{q} is the prescribed heat flux on Γ_N ; u_∞ and h_c are the temperature and the heat-transfer coefficient of the outside medium, respectively; \bar{u}^ϵ is the prescribed temperature on ∂B_ϵ , when $\alpha = 1, \beta = \gamma = 0$; \bar{q}^ϵ is the prescribed heat flux on ∂B_ϵ , when $\beta = 1, \alpha = \gamma = 0$; u_∞^ϵ and h_c^ϵ are the temperature and the heat-transfer coefficient in the interior of the channels, respectively, when $\gamma = 1, \alpha = \beta = 0$.

The problem given by Eq. (8) can be written in the variational form. In other words, this means to solve the set of Eqs. (8) in the weak sense, that is: Find $u_\epsilon \in U_\epsilon$, such that

$$a_\epsilon(u_\epsilon, w_\epsilon) = l_\epsilon(w_\epsilon) \quad \forall w_\epsilon \in V_\epsilon, \tag{11}$$

where $a_\epsilon(u_\epsilon, w_\epsilon)$ and $l_\epsilon(w_\epsilon)$ are written, respectively, as

$$a_\epsilon(u_\epsilon, w_\epsilon) = \int_{\Omega_\epsilon} k \nabla u_\epsilon \cdot \nabla w_\epsilon \, d\Omega_\epsilon + \int_{\Gamma_R} h_c u_\epsilon w_\epsilon \, d\Gamma + \gamma \int_{\partial B_\epsilon} h_c^\epsilon u_\epsilon w_\epsilon \, d\partial B_\epsilon, \tag{12}$$

$$\begin{aligned} l_\epsilon(w_\epsilon) &= \int_{\Omega_\epsilon} b w_\epsilon \, d\Omega_\epsilon - \int_{\Gamma_N} \bar{q} w_\epsilon \, d\Gamma + \int_{\Gamma_R} h_c u_\infty w_\epsilon \, d\Gamma \\ &\quad - \beta \int_{\partial B_\epsilon} \bar{q}^\epsilon w_\epsilon \, d\partial B_\epsilon + \gamma \int_{\partial B_\epsilon} h_c^\epsilon u_\infty^\epsilon w_\epsilon \, d\partial B_\epsilon \end{aligned} \tag{13}$$

and the admissible functions set U_ϵ and the admissible variations space V_ϵ are given, respectively, by

$$\begin{aligned} U_\epsilon &= \{u_\epsilon \mid u_\epsilon \in H^1(\Omega_\epsilon) : u_\epsilon|_{\Gamma_D} = \bar{u} \text{ and } \alpha u_\epsilon|_{\partial B_\epsilon} = \alpha \bar{u}^\epsilon\}, \\ V_\epsilon &= \{w_\epsilon \mid w_\epsilon \in H^1(\Omega_\epsilon) : w_\epsilon|_{\Gamma_D} = 0 \text{ and } \alpha w_\epsilon|_{\partial B_\epsilon} = 0\}, \end{aligned}$$

where $H^1(\cdot)$ is a Hilbert space of order 1 defined in a given domain. It is important to mention that, when $\alpha = 1$, $u_\epsilon|_{\partial B_\epsilon} = \bar{u}^\epsilon$ and $w_\epsilon|_{\partial B_\epsilon} = 0$; and when $\alpha = 0$, $u_\epsilon|_{\partial B_\epsilon}$ and $w_\epsilon|_{\partial B_\epsilon}$ are free on ∂B_ϵ .

The boundary value problem written in the reference configuration (Eq. 11), must also be satisfied for all perturbation τ , which can be written in the perturbed configuration Ω_τ , in the following manner: Find $u_\tau \in U_\tau := U_\epsilon(\Omega_\tau)$, such that

$$a_\tau(u_\tau, w_\tau) = l_\tau(w_\tau) \quad \forall w_\tau \in V_\tau := V_\epsilon(\Omega_\tau), \tag{14}$$

where $a_\tau(u_\tau, w_\tau)$ and $l_\tau(w_\tau)$ are given, respectively, by

$$a_\tau(u_\tau, w_\tau) = \int_{\Omega_\tau} k \nabla_\tau u_\tau \cdot \nabla_\tau w_\tau \, d\Omega_\tau + \int_{\Gamma_R} h_c u_\tau w_\tau \, d\Gamma + \gamma \int_{\partial B_{\epsilon\tau}} h_c^\epsilon u_\tau w_\tau \, d\partial B_{\epsilon\tau}, \tag{15}$$

$$\begin{aligned} l_\tau(w_\tau) &= \int_{\Omega_\tau} b w_\tau \, d\Omega_\tau - \int_{\Gamma_N} \bar{q} w_\tau \, d\Gamma + \int_{\Gamma_R} h_c u_\infty w_\tau \, d\Gamma \\ &\quad - \beta \int_{\partial B_{\epsilon\tau}} \bar{q}^\epsilon w_\tau \, d\partial B_{\epsilon\tau} + \gamma \int_{\partial B_{\epsilon\tau}} h_c^\epsilon u_\infty^\epsilon w_\tau \, d\partial B_{\epsilon\tau}, \end{aligned} \tag{16}$$

and $\epsilon_\tau = \epsilon + \tau |V_n|$ and $\nabla_\tau(\cdot)$ is adopted to denote $\nabla_\tau(\cdot) := \frac{\partial}{\partial \mathbf{x}_\tau}(\cdot)$. Observe that the boundary $\Gamma = \Gamma_N \cup \Gamma_D \cup \Gamma_R$ is fixed, as can be seen in the definition of the velocities field given by Eq. (6).

3.2 Calculus of the Topological Derivative

To obtain the expression of the Topological Derivative via Shape Sensitivity Analysis, it is necessary firstly to calculate the derivative of the cost function $\psi(\Omega_\tau) := \Psi_\tau(u_\tau)$ in relation to the parameter τ , at $\tau = 0$ (see Eq. 7). The sensitivity calculation of the cost function Ψ_τ can be realized evoking the Lagrangian Method. That is, let u_τ and λ_τ be solutions of the state and adjoint equations, respectively, then:

$$\frac{d}{d\tau} \Psi_\tau(u_\tau) = \frac{\partial}{\partial \tau} \mathcal{L}_\tau(u_\tau, \lambda_\tau) = \frac{\partial}{\partial \tau} \Psi_\tau(u_\tau) + \frac{\partial}{\partial \tau} a_\tau(u_\tau, \lambda_\tau) - \frac{\partial}{\partial \tau} l_\tau(\lambda_\tau). \quad (17)$$

where

$$\mathcal{L}_\tau(u_\tau, \lambda_\tau) = \Psi_\tau(u_\tau) + a_\tau(u_\tau, \lambda_\tau) - l_\tau(\lambda_\tau) \quad \forall \lambda_\tau \in V_\tau. \quad (18)$$

The cost function Ψ_τ is, in a certain way, arbitrary. However, to arrive at its derivative (Eq. 17) one must adopt a Ψ_τ in particular, depending on the interest and the application that one has in mind. In the heat conduction problem here under study the total potential energy is adopted as an example of objective function, which, in this case, is defined as (it is important to stand out that the methodology here proposed is not limited to this cost function in particular):

$$\begin{aligned} \Psi_\tau(u_\tau) := & \frac{1}{2} \left(\int_{\Omega_\tau} k \nabla_\tau u_\tau \cdot \nabla_\tau u_\tau \, d\Omega_\tau + \int_{\Gamma_R} h_c u_\tau^2 \, d\Gamma + \gamma \int_{\partial B_{\epsilon_\tau}} h_c^\epsilon u_\tau^2 \, d\partial B_{\epsilon_\tau} \right) \\ & - \int_{\Omega_\tau} b u_\tau \, d\Omega_\tau + \int_{\Gamma_N} \bar{q} u_\tau \, d\Gamma - \int_{\Gamma_R} h_c u_\infty u_\tau \, d\Gamma \\ & + \beta \int_{\partial B_{\epsilon_\tau}} \bar{q}^\epsilon u_\tau \, d\partial B_{\epsilon_\tau} - \gamma \int_{\partial B_{\epsilon_\tau}} h_c^\epsilon u_\infty^\epsilon u_\tau \, d\partial B_{\epsilon_\tau}. \end{aligned} \quad (19)$$

Once characterized the cost function to be studied (Eq. 19), one can calculate the derivative of the Lagrangian (Eq. 17). Thus, the adjoint equation for this particular case is given by: Find $\lambda_\tau \in V_\tau$, such that

$$\begin{aligned} a_\tau(\lambda_\tau, \dot{u}_\tau) &= - \left\langle \frac{\partial \Psi_\tau(\tau, u_\tau)}{\partial u_\tau}, \dot{u}_\tau \right\rangle \\ &= - (a_\tau(u_\tau, \dot{u}_\tau) - l_\tau(\dot{u}_\tau)) = 0 \quad \forall \dot{u}_\tau \in V_\tau, \\ &\Rightarrow \lambda_\tau = 0, \text{ see Eq. (14)}. \end{aligned} \quad (20)$$

Therefore, for u_τ and $\lambda_\tau = 0$ solutions of the state and adjoint equations (Eqs. 14, 20), respectively, the derivative of the Lagrangian (Eq. 17) remains

$$\frac{\partial}{\partial \tau} \mathcal{L}_\tau(u_\tau, u_\tau) = \frac{1}{2} \frac{\partial}{\partial \tau} a_\tau(u_\tau, u_\tau) - \frac{\partial}{\partial \tau} l_\tau(u_\tau). \quad (21)$$

The derivatives in the referential configuration $\Omega_0 = \Omega_\epsilon$ can be obtained by the Reynolds' transport theorem. Thus, the derivative of the bilinear form $a_\tau(u_\tau, u_\tau)$ becomes

$$\begin{aligned} \left. \frac{\partial a_\tau}{\partial \tau} \right|_{\tau=0} &= \int_{\Omega_\epsilon} \left[\left. \frac{\partial}{\partial \tau} (k \nabla_\tau u_\tau \cdot \nabla_\tau u_\tau) \right|_{\tau=0} + k \nabla u_\epsilon \cdot \nabla u_\epsilon \operatorname{div} \mathbf{V} \right] d\Omega_\epsilon \\ &+ \gamma \int_{\partial B_\epsilon} h_\epsilon^\epsilon u_\epsilon^2 \operatorname{div}_\Gamma \mathbf{V} d\partial B_\epsilon, \end{aligned} \tag{22}$$

where $\operatorname{div}_\Gamma \mathbf{V} = (\mathbf{I} - \mathbf{n} \otimes \mathbf{n}) \cdot \nabla \mathbf{V}$.

The derivative of the gradient of a scalar field that appears in the Eq. (22), is given by

$$\left. \frac{\partial}{\partial \tau} (\nabla_\tau u_\tau) \right|_{\tau=0} = -(\nabla \mathbf{V})^T \nabla u_\epsilon. \tag{23}$$

Substituting this last result in the Eq. (22) one has that

$$\begin{aligned} \left. \frac{\partial a_\tau}{\partial \tau} \right|_{\tau=0} &= - \int_{\Omega_\epsilon} [(\nabla \mathbf{V}^T + \nabla \mathbf{V}) k \nabla u_\epsilon \cdot \nabla u_\epsilon - k \nabla u_\epsilon \cdot \nabla u_\epsilon \operatorname{div} \mathbf{V}] d\Omega_\epsilon \\ &+ \gamma \int_{\partial B_\epsilon} h_\epsilon^\epsilon u_\epsilon^2 \operatorname{div}_\Gamma \mathbf{V} d\partial B_\epsilon. \end{aligned} \tag{24}$$

In the same way, the derivative of the functional $l_\tau(u_\tau)$ can be calculated in the following manner

$$\left. \frac{\partial l_\tau}{\partial \tau} \right|_{\tau=0} = \int_{\Omega_\epsilon} b u_\epsilon \operatorname{div} \mathbf{V} d\Omega_\epsilon - \beta \int_{\partial B_\epsilon} \bar{q}^\epsilon u_\epsilon \operatorname{div}_\Gamma \mathbf{V} d\partial B_\epsilon + \gamma \int_{\partial B_\epsilon} h_\epsilon^\epsilon u_\epsilon^\infty u_\epsilon \operatorname{div}_\Gamma \mathbf{V} d\partial B_\epsilon.$$

Thus, substituting the Eqs. (24, 3.2) in the Eq. (21) and rearranging terms, the derivative of the Lagrangian becomes

$$\left. \frac{\partial \mathcal{L}_\tau}{\partial \tau} \right|_{\tau=0} = -\frac{1}{2} \int_{\Omega_\epsilon} \boldsymbol{\Sigma} \cdot \nabla \mathbf{V} d\Omega_\epsilon + \frac{1}{2} \int_{\partial B_\epsilon} [\gamma h_\epsilon^\epsilon u_\epsilon (u_\epsilon - 2u_\epsilon^\infty) + 2\beta \bar{q}^\epsilon u_\epsilon] \operatorname{div}_\Gamma \mathbf{V} d\partial B_\epsilon,$$

where, for the problem under study, $\boldsymbol{\Sigma}$ results a symmetric tensor, given by

$$\boldsymbol{\Sigma} = 2(k \nabla u_\epsilon \otimes \nabla u_\epsilon) + (2b u_\epsilon - k \nabla u_\epsilon \cdot \nabla u_\epsilon) \mathbf{I}.$$

Since $\operatorname{div} \boldsymbol{\Sigma} = 0$, therefore, the derivative of the Lagrangian (Eq. 3.2) becomes an integral only defined on the boundary Γ_ϵ , that is,

$$\left. \frac{\partial \mathcal{L}_\tau}{\partial \tau} \right|_{\tau=0} = -\frac{1}{2} \int_{\Gamma_\epsilon} \boldsymbol{\Sigma} \mathbf{n} \cdot \mathbf{V} d\Gamma_\epsilon + \frac{1}{2} \int_{\partial B_\epsilon} [\gamma h_\epsilon^\epsilon u_\epsilon (u_\epsilon - 2u_\epsilon^\infty) + 2\beta \bar{q}^\epsilon u_\epsilon] \operatorname{div}_\Gamma \mathbf{V} d\partial B_\epsilon. \tag{25}$$

Boundary Conditions	$f(\epsilon)$	D_T
Neumann: $\beta = 1, \alpha = \gamma = 0$ and $\bar{q}^\epsilon = 0$	$-\pi\epsilon^2$	$k\nabla u \cdot \nabla u - bu$
Neumann: $\beta = 1, \alpha = \gamma = 0$ and $\bar{q}^\epsilon \neq 0$	$-2\pi\epsilon$	$-\bar{q}^\epsilon u$
Robin: $\gamma = 1, \alpha = \beta = 0$	$-2\pi\epsilon$	$-\frac{1}{2}h_c^\epsilon u (u - 2u_\infty^\epsilon)$
Dirichlet: $\alpha = 1, \beta = \gamma = 0$	$\frac{2\pi}{\log(\epsilon)}$	$-\frac{1}{2}k (u - \bar{u}^\epsilon)^2$

Table 1: Topological Derivatives for the Poisson’s problem in 2D domains

From the definition of the velocity field given by the Eq. (6) and remembering that $\epsilon_\tau = \epsilon + \tau |V_n|$ and that $\Omega_\epsilon \subset \mathbb{R}^2$, one has that $\text{div}_\Gamma \mathbf{V} = \frac{1}{\epsilon} |V_n|$. Substituting this last result in Eq. (25), taking into account the definition of the Topological Derivative obtained via Shape Sensitivity Analysis (Eq. 7) and considering that the hole is subject to an expansion ($\text{sign}(V_n) = -1$), one finally has that

$$\begin{aligned}
 D_T(\hat{\mathbf{x}}) &= \frac{1}{2} \lim_{\epsilon \rightarrow 0} \frac{1}{f'(\epsilon)} \int_{\partial B_\epsilon} \left\{ k \left(\frac{\partial u_\epsilon}{\partial n} \right)^2 - k \left(\frac{\partial u_\epsilon}{\partial t} \right)^2 + 2bu_\epsilon + \right. \\
 &\quad \left. + \frac{1}{\epsilon} [\gamma h_c^\epsilon u_\epsilon (u_\epsilon - 2u_\infty^\epsilon) + 2\beta \bar{q}^\epsilon u_\epsilon] \right\} d\partial B_\epsilon.
 \end{aligned}
 \tag{26}$$

Now, it is enough to calculate this limit with $\epsilon \rightarrow 0$ to obtain the final expression of the Topological Derivative. To do this, an asymptotic analysis shall be performed in order to know the behavior of the solution u_ϵ when $\epsilon \rightarrow 0$, as well as its normal and tangential derivatives. From this asymptotic analysis one can obtain the results shown in the Table 1 (see the works of Novotny et al.⁹ and Feijóo et al.¹¹), where one has the final expressions of the Topological Derivatives for the Poisson’s problem, taking as a cost function the total potential energy (Eq. 19) and where the solution defined in the domain Ω (without hole) is denoted by u .

From the analysis of the Table 1 one observes that it is sufficient to calculate the solution of the original problem (without hole), that is u , to obtain the sensitivity of the

cost function when a hole is created in an arbitrary point $\hat{\mathbf{x}} \in \Omega$. Thus, the Topological Derivative can be obtained without additional cost, besides that necessary in the calculation of u and λ and/or ∇u and $\nabla \lambda$ (note that in the present case $\lambda = 0$ due to the choice of a particular cost function, as can be seen in Eq. 20).

4 THE TOPOLOGICAL DERIVATIVE IN 2D ELASTICITY

Now, the Topological Derivative for 2D Elasticity problem will be presented in this section. First, it is introduced the mechanical model and further the calculus of its Topological Derivative.

4.1 Mechanical Model

Let Ω_ϵ be a deformable body, with boundary $\Gamma_\epsilon = \Gamma_N \cup \Gamma_D \cup \partial B_\epsilon$, submitted to a set of surface forces $\bar{\mathbf{q}}$ on the boundary Γ_N , body forces \mathbf{b} in the domain Ω_ϵ and displacement constraints $\bar{\mathbf{u}}$ on the boundary Γ_D . Then, the mechanical model can be described by the following variational formulation in terms of the primal variable \mathbf{u}_ϵ : Find $\mathbf{u}_\epsilon \in U_\epsilon$, such that

$$\int_{\Omega_\epsilon} \mathbf{C} \nabla^s \mathbf{u}_\epsilon \cdot \nabla^s \mathbf{w}_\epsilon \, d\Omega_\epsilon = \int_{\Omega_\epsilon} \mathbf{b} \cdot \mathbf{w}_\epsilon \, d\Omega_\epsilon + \int_{\Gamma_N} \bar{\mathbf{q}} \cdot \mathbf{w}_\epsilon \, d\Gamma_\epsilon \quad \forall \mathbf{w}_\epsilon \in V_\epsilon, \quad (27)$$

where $\nabla^s(\cdot)$ denotes the symmetric part of the gradient and \mathbf{C} is the fourth order elasticity tensor. Assuming that $\mathbf{b} \in L^2(\Omega_\epsilon)$ and $\bar{\mathbf{q}} \in L^2(\Gamma_N)$, the admissible functions set U_ϵ and the admissible variations space V_ϵ are given, respectively, by

$$U_\epsilon = \{ \mathbf{u}_\epsilon \in H^1(\Omega_\epsilon) \mid \mathbf{u}_\epsilon = \bar{\mathbf{u}} \text{ on } \Gamma_D \} \quad \text{and} \quad V_\epsilon = \{ \mathbf{w}_\epsilon \in H^1(\Omega_\epsilon) \mid \mathbf{w}_\epsilon = 0 \text{ on } \Gamma_D \} .$$

It is important to mention that on ∂B_ϵ is imposed an homogeneous Neumann condition

$$(\mathbf{C} \nabla^s \mathbf{u}_\epsilon) \mathbf{n} = \mathbf{0} \quad \text{on} \quad \partial B_\epsilon . \quad (28)$$

The variational problem written in the reference configuration must also be satisfied for all perturbation τ , that is: Find $\mathbf{u}_\tau \in U_\tau := U_\epsilon(\Omega_\tau)$, such that

$$a_\tau(\mathbf{u}_\tau, \mathbf{w}_\tau) = l_\tau(\mathbf{w}_\tau) \quad \forall \mathbf{w}_\tau \in V_\tau := V_\epsilon(\Omega_\tau) , \quad (29)$$

where $a_\tau(\mathbf{u}_\tau, \mathbf{w}_\tau)$ and $l_\tau(\mathbf{w}_\tau)$ are given, respectively, by

$$a_\tau(\mathbf{u}_\tau, \mathbf{w}_\tau) = \int_{\Omega_\tau} \mathbf{C} \nabla_\tau^s \mathbf{u}_\tau \cdot \nabla_\tau^s \mathbf{w}_\tau \, d\Omega_\tau \quad \text{and} \quad l_\tau(\mathbf{w}_\tau) = \int_{\Omega_\tau} \mathbf{b} \cdot \mathbf{w}_\tau \, d\Omega_\tau + \int_{\Gamma_N} \bar{\mathbf{q}} \cdot \mathbf{w}_\tau \, d\Gamma_\tau .$$

4.2 Calculus of the Topological Derivative

In this work, considering the wide range of engineering applications, it is also adopted as cost function the total potential energy

$$\psi(\Omega_\tau) := \frac{1}{2} a_\tau(\mathbf{u}_\tau, \mathbf{u}_\tau) - l_\tau(\mathbf{u}_\tau) . \quad (30)$$

The derivative of the cost function in relation to τ , at $\tau = 0$, is given by^{8,10}

$$\left. \frac{d}{d\tau} \psi(\Omega_\tau) \right|_{\tau=0} = \int_{\Omega_\epsilon} \boldsymbol{\Sigma} \cdot \nabla \mathbf{V} \, d\Omega_\epsilon, \quad (31)$$

where $\boldsymbol{\Sigma}$ is the Energy-Momentum Tensor introduced by Eshelby, when he studied defects in the context of infinitesimal deformations of elastic bodies^{17,18}, written as

$$\boldsymbol{\Sigma} = \frac{1}{2} (\mathbf{C} \nabla^s \mathbf{u}_\epsilon \cdot \nabla^s \mathbf{u}_\epsilon) \mathbf{I} - (\mathbf{b} \cdot \mathbf{u}_\epsilon) \mathbf{I} - \nabla \mathbf{u}_\epsilon^T (\mathbf{C} \nabla^s \mathbf{u}_\epsilon). \quad (32)$$

Since $\text{div} \boldsymbol{\Sigma} = 0$ when the equilibrium holds, then recalling the divergence theorem and considering the velocity field given by Eq. (6), the derivative of the cost function becomes

$$\left. \frac{d}{d\tau} \psi(\Omega_\tau) \right|_{\tau=0} = \int_{\Gamma_\epsilon} \boldsymbol{\Sigma} \mathbf{n} \cdot \mathbf{V} \, d\Gamma_\epsilon = V_n \int_{\partial B_\epsilon} \boldsymbol{\Sigma} \mathbf{n} \cdot \mathbf{n} \, d\partial B_\epsilon. \quad (33)$$

Taking into account that

$$\boldsymbol{\Sigma} \mathbf{n} \cdot \mathbf{n} = \frac{1}{2} (\mathbf{C} \nabla^s \mathbf{u}_\epsilon \cdot \nabla^s \mathbf{u}_\epsilon) - \mathbf{b} \cdot \mathbf{u}_\epsilon - (\mathbf{C} \nabla^s \mathbf{u}) \mathbf{n} \cdot (\nabla \mathbf{u}_\epsilon) \mathbf{n},$$

and remembering that $(\mathbf{C} \nabla^s \mathbf{u}) \mathbf{n} = 0$ on ∂B_ϵ (see Eq. 28), then the Eq. (33) simplifies as following,

$$\left. \frac{d}{d\tau} \psi(\Omega_\tau) \right|_{\tau=0} = V_n \int_{\partial B_\epsilon} \left(\frac{1}{2} \mathbf{C} \nabla^s \mathbf{u}_\epsilon \cdot \nabla^s \mathbf{u}_\epsilon - \mathbf{b} \cdot \mathbf{u}_\epsilon \right) \, d\partial B_\epsilon. \quad (34)$$

Finally, substituting the Eq. (34) in the result of the TSSA Theorem (7) and considering an expansion on the hole ($\text{sign}(V_n) = -1$), it is obtained

$$D_T(\hat{\mathbf{x}}) = \lim_{\epsilon \rightarrow 0} \frac{1}{f'(\epsilon)} \int_{\partial B_\epsilon} \left(\frac{1}{2} \mathbf{C} \nabla^s \mathbf{u}_\epsilon \cdot \nabla^s \mathbf{u}_\epsilon - \mathbf{b} \cdot \mathbf{u}_\epsilon \right) \, d\partial B_\epsilon, \quad (35)$$

Now, analogous to the Poisson's case, an asymptotic analysis was performed in order to know the behavior of the solution \mathbf{u}_ϵ , as well as the associated deformation $\nabla^s \mathbf{u}_\epsilon$, when $\epsilon \rightarrow 0$. Then, for an isotropic linear elastic material and null body forces ($\mathbf{b} = \mathbf{0}$), the Topological Derivative obtained from this asymptotic analysis is given by:

- **Plane Strain**

$$D_T(\hat{\mathbf{x}}) = 2(1 - \nu) \mathbf{T} \cdot \nabla^s \mathbf{u} + \frac{(1 - \nu)(4\nu - 1)}{2(1 - 2\nu)} \text{tr} \mathbf{T} \, \text{tr} \nabla^s \mathbf{u} \quad (36)$$

- **Plane Stress**

$$D_T(\hat{\mathbf{x}}) = \frac{2}{1 + \nu} \mathbf{T} \cdot \nabla^s \mathbf{u} + \frac{(3\nu - 1)}{2(1 - \nu^2)} \text{tr} \mathbf{T} \, \text{tr} \nabla^s \mathbf{u} \quad (37)$$

where $\mathbf{u}(\hat{\mathbf{x}})$ is the solution defined in the original domain Ω (without hole) and $\mathbf{T} = \mathbf{C} \nabla^s \mathbf{u}$ is the corresponding stress. It is interesting to remark that the same solution was obtained by Garreau et. al.⁵ using the Domain Truncation Method.

5 APPLICATION IN THE TOPOLOGICAL OPTIMIZATION CONTEXT

In this Section, the Topological Derivative obtained through the Shape Sensitivity Analysis (see the expression (7)) shall be utilized for the determination of the optimal topology in several problems of heat conduction and 2D elasticity. In all examples, the total potential energy is adopted as cost function and, as a constraint, the state equation in its weak (variational) form. However, the topological optimization problem is, in general, more complex. In fact, it is still necessary to consider some additional constraint in the problem, besides the state equation, in order to avoid that any topological optimization algorithm to be developed leads merely to the trivial solution of the problem, *i.e.* $meas(\Omega) = 0$. Nevertheless, in the manner as presented in this work, a simple way to outline this problem consists in introducing a stop criteria in the algorithm, that can be, for instance, over the final volume to be obtained. That is, the idea is creating the holes while $meas(\Omega) \geq meas(\hat{\Omega})$, where $meas(\hat{\Omega})$ corresponds to the final volume required. Thus, considering this stop criteria, a proposal of a topological optimization algorithm based on the Topological Derivative may be summarized on the following steps (in the work of C ea et al.⁷ one can find a variation of this algorithm):

A topological optimization algorithm

Considering the following sequence $\{\Omega^j \mid meas(\Omega^j) \geq meas(\hat{\Omega})\}$, where j is the j -th iteration, then:

1. Provide the initial domain Ω^0 and the constraint $meas(\hat{\Omega})$.
2. While $meas(\Omega^j) \geq meas(\hat{\Omega})$ do:
 - (a) Find the solution w^j associated to the domain Ω^j .
 - (b) Calculate $D_T(\hat{\mathbf{x}})^j$ according to Table (1), (36) or (37).
 - (c) Create the holes in the points $\hat{\mathbf{x}}$ corresponding to $\eta_{inf}^j \leq D_T(\hat{\mathbf{x}})^j \leq \eta_{sup}^j$, where η_{inf}^j and η_{sup}^j are specified proportional to the volume of material to be removed in each iteration j .
 - (d) Define the new domain Ω^{j+1} .
 - (e) Make $j \leftarrow j + 1$.
3. At this stage, it is hoped to have in hand the desired final topology.

Although the algorithm is simple and rudimentary, even so it is possible to obtain satisfactory results. However, other algorithms could be proposed in order to use better the information contained in the Topological Derivative.

5.1 Numerical results

For the problems studied in this paper, the Topological Derivative depends on $u(\hat{\mathbf{x}})$ and/or $\nabla u(\hat{\mathbf{x}})$, the source b and the boundary conditions on ∂B_ϵ . In this work, the solution $u(\hat{\mathbf{x}})$ is calculated via the Finite Element Method^{19–21}, that is, $u(\hat{\mathbf{x}}) \approx u_h(\hat{\mathbf{x}})$ and $\nabla u(\hat{\mathbf{x}}) \approx \nabla u_h(\hat{\mathbf{x}})$, where $\nabla u_h(\hat{\mathbf{x}})$ is obtained by a post-processing²² of the approximated solution $u_h(\hat{\mathbf{x}})$. More specifically, in the following examples the three node triangular finite element is adopted for the discretization of the variational problem^{20,21}. Furthermore, $D_T(\hat{\mathbf{x}})$ is evaluated at the nodal points of the finite elements mesh, being that the elements that share the node which satisfies $\eta_{\text{inf}} \leq D_T(\hat{\mathbf{x}}) \leq \eta_{\text{sup}}$ are eliminated (for more technical details see the work of Novotny²³).

5.1.1 Example 1 - a heat exchanger

The problem being considered can be seen in Fig. 1, where one has a body denoted by Ω , whose thermal conductivity is such that $k = 204W/(m^\circ C)$, and a cooling surface, Γ_R , which is exposed to the ambient air (steady air) at a temperature $u_\infty = 25^\circ C$, leading to a heat-transfer coefficient $h_c = 20W/(m^2^\circ C)$. When a cooling channel (hole) is introduced, one has water at a temperature $u_\infty^c = 30^\circ C$, that flows throughout the interior of it, in order to induce a heat-transfer coefficient $h_c^c = 200W/(m^2^\circ C)$ (Neumann or Dirichlet boundary conditions on ∂B_ϵ are very severe hypothesis, the reason for which only the Robin boundary conditions shall be imposed on ∂B_ϵ). Finally, the heat flux \bar{q} prescribed on Γ_N presents a piecewise linear distribution, where the smallest value is $\bar{q}_1 = 2 \times 10^3W/m^2$ and the greatest value is $\bar{q}_2 = 2 \times 10^4W/m^2$. Due to the periodical symmetry of the problem, only a part $2L \times L$, where $L = 4m$, of the whole domain is discretized (see mesh shown in Fig. 1), and the gray region of width $a = 1m$ each one, shown in the same figure, shall not be optimized, being considered the structural part of the problem.

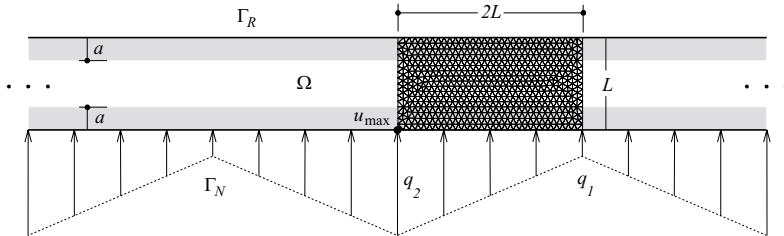


Figure 1: Example 1 - model and mesh with 1086 finite elements of a heat exchanger.

By creating the holes where $D_T(\hat{\mathbf{x}}) \approx \frac{1}{2}h_c^c u_h(\hat{\mathbf{x}})(u_h(\hat{\mathbf{x}}) - 2u_\infty^c)$ (see Table 1, Robin b.c.) assumes the **greatest** absolute values, the maximum temperature, denoted by u_{max} in

Fig. 1, should be rapidly diminished up to the required value u_{\max}^* . The idea, therefore, is to accomplish a topological optimization of the structure for now described up to $u_{\max} \leq u_{\max}^*$. Considering this new stop criteria in the algorithm, with $u_{\max}^* = 200^\circ C$ and removing 1% of the material in each iteration, one observes that the temperature u_{\max} actually diminishes during the iterative process, which can be seen in Fig. 2.

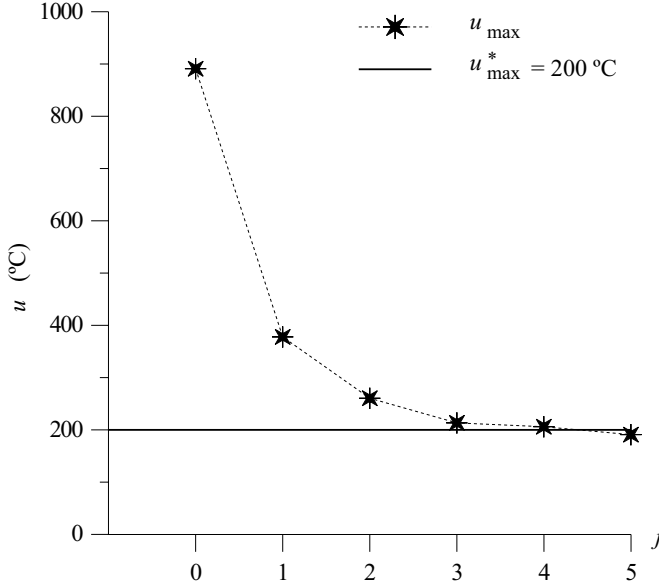


Figure 2: Example 1 - maximum temperature (u_{max}) in each iteration.

Through analysis of Fig. 2, one notes that the condition $u_{\max} < u_{\max}^*$ is reached in the iteration $j = 5$, from which u_{\max} presents an asymptotic behavior. Thus, if the required temperature were $u_{\max}^* \ll 200^\circ C$ ($u_{\max}^* = 100^\circ C$, for instance), the flow condition imposed into the cooling channels (represented by the parameters h_c^ϵ and u_∞^ϵ) would be insufficient to reach it.

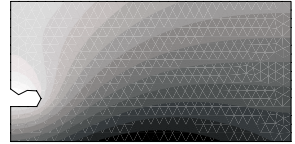
The temperature distribution obtained in each iteration is shown in Fig. 3, where one observes a diminution of the temperature in the whole domain, as the cooling channels are being automatically introduced via Topological Derivative, whose distribution calculated in each iteration can be seen in Fig. 4.

Field: U-1
 Max.: 8.910951E+002
 Node: 201
 Min.: 5.438589E+002
 Node: 505
 Palette:
 8.910951E+002
 8.693928E+002
 8.476906E+002
 8.259883E+002
 8.042860E+002
 7.825838E+002
 7.608815E+002
 7.391792E+002
 7.174770E+002
 6.957747E+002
 6.740724E+002
 6.523702E+002
 6.306679E+002
 6.089656E+002
 5.872634E+002
 5.655611E+002
 5.438589E+002



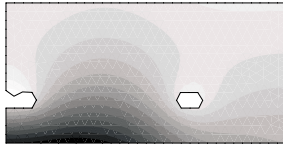
(a) temperature at $j = 0$

Field: U-1
 Max.: 3.777495E+002
 Node: 377
 Min.: 1.134470E+002
 Node: 93
 Palette:
 3.777495E+002
 3.612305E+002
 3.447115E+002
 3.281927E+002
 3.116738E+002
 2.951549E+002
 2.786360E+002
 2.621171E+002
 2.455982E+002
 2.290793E+002
 2.125604E+002
 1.960415E+002
 1.795226E+002
 1.630037E+002
 1.464848E+002
 1.299659E+002
 1.134470E+002



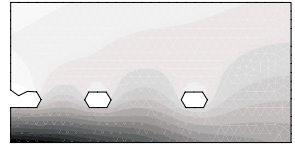
(b) temperature at $j = 1$

Field: U-1
 Max.: 2.605044E+002
 Node: 267
 Min.: 8.073090E+001
 Node: 93
 Palette:
 2.605044E+002
 2.492703E+002
 2.380362E+002
 2.267921E+002
 2.155580E+002
 2.043239E+002
 1.930898E+002
 1.818557E+002
 1.706216E+002
 1.593875E+002
 1.481534E+002
 1.369193E+002
 1.256852E+002
 1.144511E+002
 1.032170E+002
 9.198329E+001
 8.073090E+001



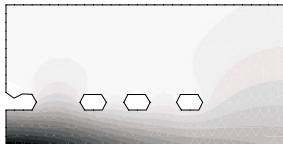
(c) temperature at $j = 2$

Field: U-1
 Max.: 2.132322E+002
 Node: 201
 Min.: 5.836520E+001
 Node: 93
 Palette:
 2.132322E+002
 2.035529E+002
 1.938737E+002
 1.841944E+002
 1.745152E+002
 1.648360E+002
 1.551568E+002
 1.454776E+002
 1.357984E+002
 1.261192E+002
 1.164400E+002
 1.067608E+002
 9.708193E+001
 8.740274E+001
 7.772355E+001
 6.804436E+001
 5.836520E+001



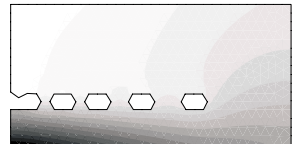
(d) temperature at $j = 3$

Field: U-1
 Max.: 2.058692E+002
 Node: 201
 Min.: 5.308980E+001
 Node: 93
 Palette:
 2.058692E+002
 1.962204E+002
 1.867171E+002
 1.772238E+002
 1.677305E+002
 1.582372E+002
 1.487439E+002
 1.392506E+002
 1.297573E+002
 1.202640E+002
 1.107707E+002
 1.012774E+002
 9.178401E+001
 8.234028E+001
 7.289655E+001
 6.345282E+001
 5.308980E+001



(e) temperature at $j = 4$

Field: U-1
 Max.: 1.907056E+002
 Node: 201
 Min.: 4.139383E+001
 Node: 93
 Palette:
 1.907056E+002
 1.813755E+002
 1.720454E+002
 1.627153E+002
 1.533852E+002
 1.440551E+002
 1.347250E+002
 1.253949E+002
 1.160648E+002
 1.067347E+002
 9.740346E+001
 8.807335E+001
 7.874324E+001
 6.941313E+001
 6.008302E+001
 5.075291E+001
 4.139383E+001



(f) temperature at $j = 5$

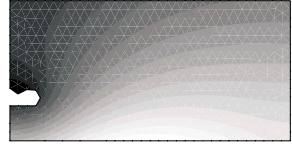
Figure 3: Example 1 - temperature distribution obtained during the iterative process.

Field: GradTop-1
 Max.: -2.631509E+007
 Node: 805
 Min.: -7.405847E+007
 Node: 201
 Palette:
 -2.631509E+007
 -2.92905E+007
 -3.228301E+007
 -3.526698E+007
 -3.823094E+007
 -4.123490E+007
 -4.421886E+007
 -4.720282E+007
 -5.018678E+007
 -5.317074E+007
 -5.615471E+007
 -5.913867E+007
 -6.212263E+007
 -6.510659E+007
 -6.809055E+007
 -7.107451E+007
 -7.405847E+007



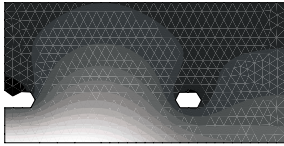
(a) Topological Derivative at $j = 0$

Field: GradTop-1
 Max.: -6.063402E+005
 Node: 93
 Min.: -1.200297E+007
 Node: 377
 Palette:
 -5.063402E+005
 -3.318623E+006
 -2.030912E+006
 -2.743206E+006
 -1.405455E+006
 -1.187784E+006
 -8.880073E+005
 -5.923631E+005
 -6.304650E+005
 -7.016939E+005
 -7.729228E+005
 -8.441516E+005
 -9.153805E+005
 -9.866094E+005
 -1.057838E+006
 -1.128967E+006
 -1.200297E+007



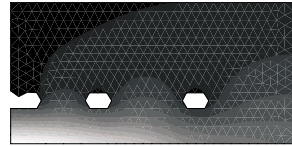
(b) Topological Derivative at $j = 1$

Field: GradTop-1
 Max.: -1.476324E+005
 Node: 93
 Min.: -5.23321E+006
 Node: 267
 Palette:
 -1.476324E+005
 -4.833598E+005
 -7.993571E+005
 -1.11354E+006
 -1.431352E+006
 -1.747399E+006
 -2.063347E+006
 -2.379344E+006
 -2.695341E+006
 -3.011339E+006
 -3.327336E+006
 -3.643333E+006
 -3.959331E+006
 -4.275328E+006
 -4.591325E+006
 -4.907323E+006
 -5.223320E+006



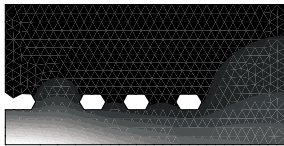
(c) Topological Derivative at $j = 2$

Field: GradTop-1
 Max.: 9.541822E+003
 Node: 93
 Min.: -5.267402E+006
 Node: 201
 Palette:
 541822E+003
 -1.952672E+005
 -1.000762E+005
 -6.04862E+004
 -9.096942E+004
 -1.014503E+006
 -1.239312E+006
 -1.424121E+006
 -1.628930E+006
 -1.833739E+006
 -2.038548E+006
 -2.243357E+006
 -2.448166E+006
 -2.652975E+006
 -2.857784E+006
 -3.062593E+006
 -3.267402E+006



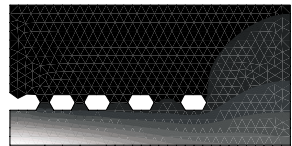
(d) Topological Derivative at $j = 3$

Field: GradTop-1
 Max.: 3.668610E+004
 Node: 93
 Min.: -3.002999E+006
 Node: 201
 Palette:
 3.668610E+004
 -1.53294E+005
 -3.432745E+005
 -5.332548E+005
 -7.232351E+005
 -9.132154E+005
 -1.103195E+006
 -1.293176E+006
 -1.483156E+006
 -1.673137E+006
 -1.863117E+006
 -2.053097E+006
 -2.243077E+006
 -2.433058E+006
 -2.623038E+006
 -2.813018E+006
 -3.002999E+006



(e) Topological Derivative at $j = 4$

Field: GradTop-1
 Max.: 7.701806E+004
 Node: 93
 Min.: -2.492630E+006
 Node: 201
 Palette:
 7.701806E+004
 -3.38447E+004
 -2.441880E+005
 -1.047910E+005
 -6.53991E+005
 -7.239971E+005
 -8.866021E+005
 -1.047203E+006
 -1.207866E+006
 -1.368408E+006
 -1.529012E+006
 -1.689616E+006
 -1.850218E+006
 -2.010821E+006
 -2.171424E+006
 -2.332027E+006
 -2.492630E+006



(f) Topological Derivative at $j = 5$

Figure 4: Example 1 - Topological Derivative obtained during the iterative process.

The final topology obtained in the iteration $j = 5$ is presented in Fig. 5, where one notes that the distance between the channels grows as these stand back from the point of maximum temperature, as it was expected.

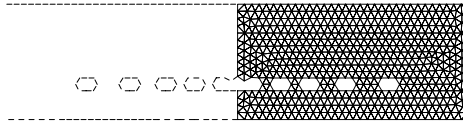


Figure 5: Example 1 - final topology.

This example shows, therefore, how the Topological Derivative can be utilized to optimize the topology of heat exchangers, in order to automatically determinate where the cooling channels must be positioned, satisfying some design requirement.

5.1.2 Example 2 - a bicycle

This example shows how Topological Derivative can be used in order to suggest a new design to a classical product: a bicycle. The Fig. 6a presents the *lay-out* of a common bicycle superposed to the initial configuration to be optimized. The Young's modulus $E = 210 \times 10^3 \text{ MPa}$, Poisson's ratio $\nu = 1/3$ and thickness $\rho = 5 \text{ mm}$ are assumed. The final topology, considering $\text{meas}(\hat{\Omega}) = 0.30\text{meas}(\Omega)$, is shown in Fig. 6b, where 1% of material was removed at each iteration.

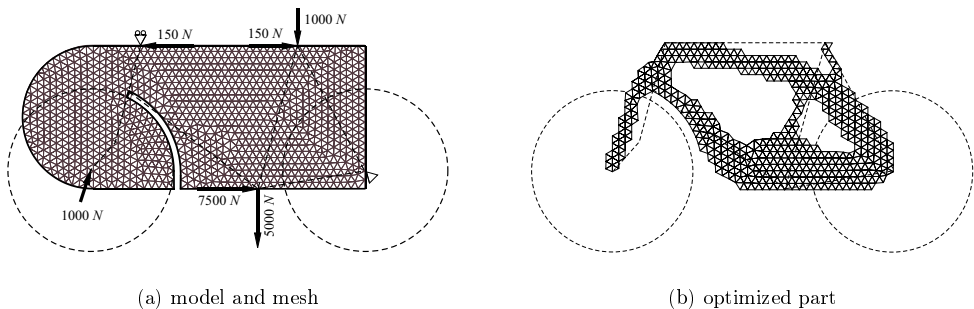


Figure 6: Example 2 - inicial and final topology.

In Fig. 6b is shown an overlap between the final result and a classical bicycle design. One can observe that the result obtained by topological optimization remain close to the usual design of a bicycle: this is probably due to the large empirical knowledge included in this type of vehicle.

5.1.3 Example 3 - a cantilever beam

The design of a cantilever beam is performed. The model is shown in Fig. 7.a, where the initial domain is represented by a square panel $\Omega = (0, 50) \times (0, 50) \text{ mm}^2$, whose

thickness is $\rho = 5 \text{ mm}$, clamped in the region denoted by $a = 5 \text{ mm}$ and submitted to a concentrated load $F = 5000 \text{ N}$, also Young's modulus $E = 210 \times 10^3 \text{ MPa}$ and Poisson's ratio $\nu = 1/3$ are assumed. In the topological optimization process, 1% of material shall be removed at each iteration. This problem is discretized into 3656 finite elements, as shown in Fig. 7.b. The final topology, considering $meas(\hat{\Omega}) = 0.42meas(\Omega)$, is obtained at iteration $j = 53$, where one has a quite classical solution (see Fig. 7c).

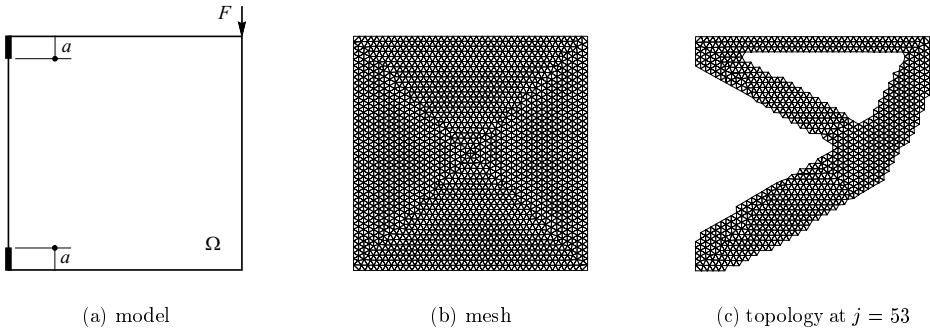


Figure 7: Example 3 - a cantilever beam design.

5.1.4 Example 4 - a Michell structure

The design of a Michell structure is performed. In Fig. 8 is shown the initial domain given by a simply supported rectangular panel $\Omega = (0, 50) \times (0, 100) \text{ mm}^2$ with thickness $\rho = 5 \text{ mm}$, submitted to a concentrated load $F = 5000 \text{ N}$. The material properties are given by $E = 210 \times 10^3 \text{ MPa}$ and Poisson's ratio $\nu = 1/3$. Considering the symmetry of the problem, the panel is discretized into 3656 finite elements.

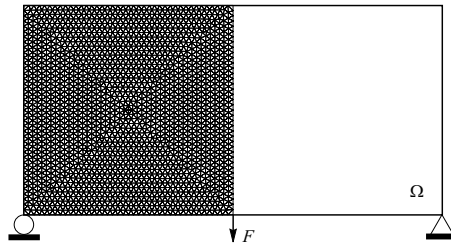


Figure 8: Example 4 - a Michell structure design.

Taking $meas(\hat{\Omega}) = 0.22meas(\Omega)$, the final topology is obtained at iteration $j = 67$, as can be seen in Fig. 9, where one has a classical Michell structure.

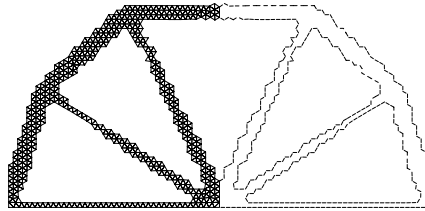


Figure 9: Example 4 - topology at $j = 67$.

5.1.5 Example 5 - a short beam

Now, the design of simply supported short beam, submitted to a concentrated load $F = 5000 N$, is performed. The elastic material properties are given by $E = 210 \times 10^3 MPa$ and $\nu = 1/3$. The initial domain $\Omega = (0, 50) \times (0, 150) mm^2$, with $\rho = 5 mm$, is discretized, considering the symmetry of the problem, into 5494 finite elements (see Fig. 10).

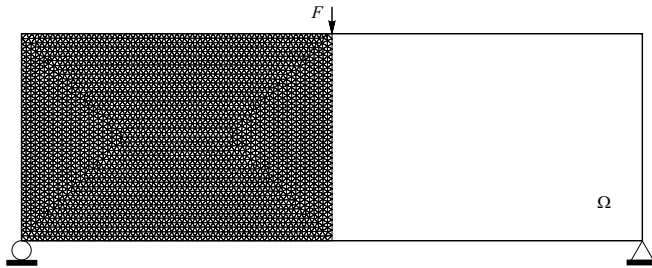


Figure 10: Example 5 - a short beam design.

The final result obtained from the topological optimization procedure is depicted in Fig. 11. This result was obtained at iteration $j = 69$ considering $meas(\hat{\Omega}) = 0.23meas(\Omega)$.

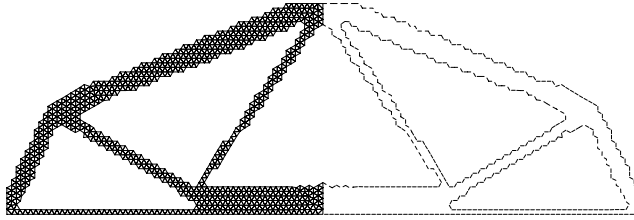


Figure 11: Example 5 - topology at $j = 69$.

5.1.6 Example 6 - a bridge structure

In this last example, the design of a bridge is considered. The model is shown in Fig. 12, where one has the initial domain represented by a rectangular panel $\Omega = (0, 60) \times (0, 180)$ m^2 , whose thickness $\rho = 0.3$ m , under a uniformly distributed traffic loading $q = 250 \times 10^3$ N/m^2 applied on the grey strip positioned at $c = 30$ m from the top of the design domain (this strip of height $b = 3$ m will not be optimized). Finally, the material properties are given by $E = 210 \times 10^3$ MPa and $\nu = 1/3$. The panel is clamped on the region $a = 9$ m and simply support on the extremes of the gray strip (a similar example can be found by Q.Q. Liang and G.P. Steven²⁴).

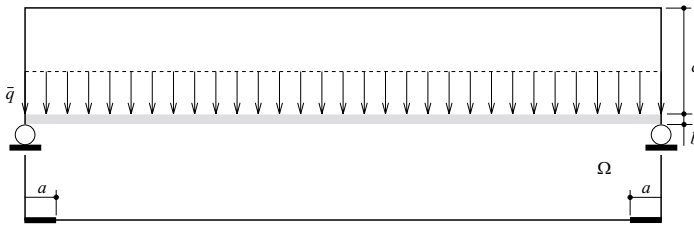


Figure 12: Example 6 - a bridge structure design.

Considering the symmetry of the problem, the initial domain is discretized into 5470 finite elements, whose mesh is shown in Fig. 13.a. The topology optimization history can be seen in Fig. (13b-d) at $j = 23$, 33 and 43, respectively.

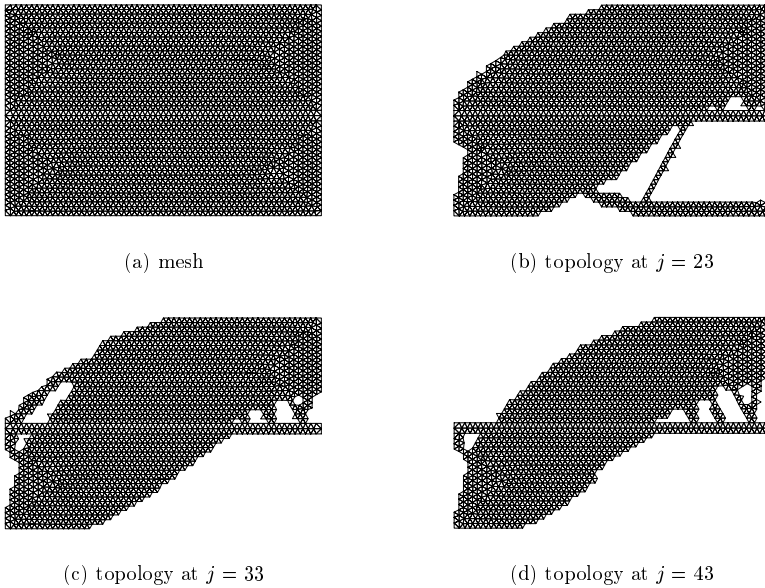


Figure 13: Example 6 - topology optimization history.

The final topology, considering $meas(\hat{\Omega}) = 0.32meas(\Omega)$, is obtained at iteration $j = 63$, where one can observe a well-known tie-arch bridge structure, as shown in Fig. 14.

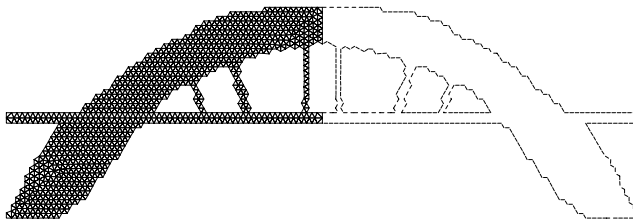


Figure 14: Example 6 - topology at $j = 63$.

A result obtained from a finer mesh (the initial domain is discretized into 21984 finite elements) is shown in Fig. 15, where one can observe that the final topology is slice different from the one shown in Fig. 14.

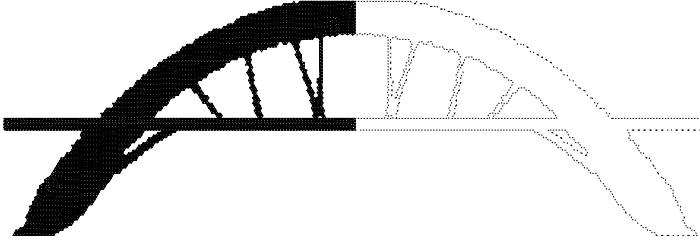


Figure 15: Example 6 - topology at $j = 71$ (finer mesh).

It is important to mention that the above result was obtained at iteration $j = 71$ considering $meas(\hat{\Omega}) = 0.25meas(\Omega)$.

6 CONCLUSIONS

In this work, Shape Sensitivity Analysis was employed to calculate the Topological Derivative. The relationship between both concepts was formally demonstrated by the authors^{9,11}. The TSSA Theorem (see expression (7)) shows that the Topological Derivative is a generalization of the Shape Sensitivity Analysis concept. Therefore, results obtained in Shape Sensitivity Analysis can be used to calculate the Topological Derivative in a simple and constructive way as shown in Section 3 and Section 4.

In order to illustrate the potentialities of the result obtained by the TSSA Theorem, the Topological Derivative was calculated, utilizing the expression (7), for steady-state heat conduction and 2D elasticity problems taking as cost function the total potential energy. These are adequate examples, since has several practical applications allowing the study of the effects on the theory due to different boundary conditions on the hole (Dirichlet, Neumann or Robin boundary conditions).

It is important to mention that the extension of the methodology here proposed to other engineering problems (non-linear Solid Mechanics, Fluid Mechanics, Electromagnetism, and so on) with general cost functions is straightforward.

The Topological-Shape Sensitivity Analysis, *i.e.* the Topological Derivative calculated via Shape Sensitivity Analysis, was expressed in terms of the limit $\epsilon \rightarrow 0$ in expression (7). To calculate this limit, it was necessary to make an asymptotic analysis of the solution u_ϵ and of its normal and tangential derivatives, which allowed to apply the localization theorem to obtain the results shown in Table 1 and expressions (36)-(37). However, when it is not possible to perform an asymptotic analysis of the solution, the limit can be estimated numerically allowing to extend the methodology proposed in this work to more complex problems.

Finally, in Section 5, the proposed topological optimization algorithm based on the Topological Sensitivity Analysis concept, led to excellent results, even though it was implemented in a rudimentary way. This highlights the potentialities of the Topological

Derivative concept when applied to topology optimization. However, other strategies using the information provided by Topological-Shape Sensitivity Analysis must be explored. Among those, an strategy that exploits the eigenvectors of the tensor Σ will be studied in future works.

Acknowledgements

This research was partly supported by FINEP/CNPq-PRONEX (Brazil) Project under Contract 664007/1997-0, by MCT/PCI-LNCC Project and by CONICET (Argentina). Antonio André Novotny was partially supported by Brazilian government fellowship from CNPq under Grant 141560/2000-2. The support from these agencies is greatly appreciated.

REFERENCES

- [1] M.P. Bendsøe & N. Kikuchi, Generating Optimal Topologies in Structural Design Using an Homogenization Method, *Comput. Methods Appl. Mech. Engrg.*, 71, 197-224, 1988.
- [2] J.E. Souza de Cursi, Allégement d'une Pièce Élastique Homogène Soumise à des Contraintes Planes, Research Report n. 1/94, L.M.R. Rouen - France, 1994.
- [3] A. Schumacher, *Topologieoptimierung von Bauteilstrukturen unter Verwendung von Lochpositionierungskriterien*, Ph.D. Thesis, Universität-Gesamthochschule-Siegen, Siegen, 1995.
- [4] S. Garreau, Ph. Guillaume & M. Masmoudi, *The Topological Gradient*, Research Report, UFR MIG, Université Paul Sabatier Toulouse 3, France 1998.
- [5] S. Garreau, Ph. Guillaume & M. Masmoudi, *The Topological Asymptotic for PDE Systems: The Elasticity Case*, *SIAM J. Control. Optim.*, Vol.39, No.6, 1756-1778, 2001.
- [6] J. Sokolowski & A. Zochowski, *On Topological Derivative in Shape Optimization*, Research Report n. 3170, INRIA-Lorraine, France, 1997.
- [7] J. Céa, S. Garreau, Ph. Guillaume & M. Masmoudi, *The Shape and Topological Optimizations Connection*, *Comput. Methods. Appl. Mech. Engrg.*, Vol. 188, 713-726, 2000. See also: Research Report, UFR MIG, Université Paul Sabatier Toulouse 3, France, 1998.
- [8] A.A. Novotny, R.A. Feijóo, C. Padra & E. Taroco, *Derivada Topológica via Análise de Sensibilidade à Mudança de Forma na Otimização Topológica*. To appear on *Revista Internacional sobre Métodos Numéricos para Cálculo y Diseño en Ingeniería*, 2002.
- [9] A.A. Novotny, R.A. Feijóo, C. Padra & E. Taroco, *Topological Sensitivity Analysis*. Submitted to *Comput. Methods Appl. Mech. Engrg.* See also LNCC Research Report N^o17/2002, Brasil, 2002.
- [10] A.A. Novotny, R.A. Feijóo, C. Padra & E. Taroco, *Topological Optimization via Shape Sensitivity Analysis Applied to 2D Elasticity*, Fifth World Congress on Computa-

- tional Mechanics, July 7-12, Vienna, Austria, 2002.
- [11] R.A. Feijóo, A.A. Novotny, C. Padra & E. Taroco, *The Topological Derivative for the Poisson's Problem*. Submitted to Math. Models and Methods in Applied Science. See also LNCC Research Report N^o16/2002, Brasil, 2002.
 - [12] J.P. Zolézio, *The Material Derivative (or Speed) Method for Shape Optimization*. In Optimization of Distributed Parameters Structures, Iowa, 1981.
 - [13] M.E. Gurtin, *An Introduction to Continuum Mechanics*, Mathematics in Science and Engineering, Academic Press, New York, 1981.
 - [14] F. Murat & J. Simon, *Sur le Controle par un Domaine Geometrique*, Ph.D. Thesis, Universite P. et M. Curie (Paris VI), Paris, France, 1976.
 - [15] D.E. Carlson, Linear Thermoelasticity, Handbuch der Physik, Band VIa/2, Springer-Verlag, 1972.
 - [16] J.C. Slattery, Advanced Transport Phenomena, McGraw Hill, 1997.
 - [17] J.D. Eshelby, *The Elastic Energy-Momentum Tensor*, Journal of Elasticity, 5, 321-335, 1975.
 - [18] E. Taroco, G. Buscaglia and R.A. Feijóo, *Second Order Shape Sensitivity Analysis for Non-Linear Problems*, Int. J. for Structural Optimization, 15-2, 101-113, 1998.
 - [19] B. Szabó & I. Babuška, *Finite Element Analysis*, John Wiley & Sons, New York, 1991.
 - [20] O.C. Zienkiewicz & R. L. Taylor, *The Finite Element Method*, vols. 1 and 2, McGraw Hill, 1989.
 - [21] T.J.R. Hughes, *The Finite Element Method - Linear Static and Dynamic Finite Element Analysis*, Prentice-Hall, New Jersey, 1987.
 - [22] E. Hinton & J.S. Campbell, Local and Global Smoothing of Discontinuous Finite Element Functions Using a Least Square Method, Int. J. Num. Methods Engrg., 8, 461-480, 1974.
 - [23] A.A. Novotny, Adaptividade h na Otimização Topológica e Projeto Ótimo de Malhas hp Adaptativas, Master Thesis, GRANTE-EMC-UFSC, Florianópolis - Brasil, 1998.
 - [24] Q.Q. Liang & G.P. Steven, *A Performance-Based Optimization Method for Topology Design of Continuum Structures with Mean Compliance Constraint*, Comp. Methods Appl. Mech. Engrg., 191, 1471-1489, 2002.